

Cloaked Resonant States in Bilayer Graphene

A. V. Shytov

School of Physics, University of Exeter,

Stoker Rd, Exeter, EX4 4QL, United Kingdom

Abstract

Charge carriers in bilayer graphene occupy two parabolic continua of electron-like and hole-like states which differ by the alignment between carrier pseudospin and its momentum, the property known as chirality. Due to chirality conservation, a strong confining potential can host unusual bound states: electron levels cloaked into the hole continuum. The energy levels and the wave functions of the cloaked states can be obtained by solving the Schrödinger equation for a massive non-chiral particle in the p -wave channel in two dimensions. Eventually, cloaked states slowly decay into the continuum, via trigonal warping effects. We discuss the key properties of cloaked states in circularly symmetric potentials, and show that cloaking should be observable in quantum corral geometries via scanning tunneling probe measurements.

There are two related fundamental facts that make the electronic properties of graphene interesting: the coexistence of electron and hole states in the vicinity of conic points in the spectrum, and chirality of charge carriers. Charge carriers in graphene can be characterized by their pseudospin, and different alignments between pseudospin and momentum result in electron-like and hole-like states. There is an important difference between the cases of monolayer and bilayer graphene (BLG) due to their different dispersion laws and different structure of chiral states. In single-layer graphene, the linear dispersion results in the density of states vanishing at the Dirac point [1]. In bilayer graphene, the dispersion is parabolic, and the density of states is flat [2], so that there is a large number of both electron- and hole-like states near the point separating the two subbands. One consequence of this is a potential instability of bilayer graphene with respect to formation of broken-symmetry phases [3]. The chirality also affects transport properties. In monolayer graphene, any potential barrier is perfectly transparent at normal incidence [4]. In bilayer graphene, chirality is responsible for electron cloaking [5] described below.

The effects of chirality are manifested in the properties of bound and quasi-bound states. In monolayer graphene, a strong confining potential, such as the supercritical Coulomb potential[6], can give rise to a quasi-localized resonance which was recently observed in scanning tunneling microscopy (STM) experiments[7]. The resonant state is formed by electron-like states submerged into the hole band and coupled to it via Klein tunneling. The number of states available for decay is suppressed by linear density of states, so that the width of the resonant peak is smaller than its energy, and the resonance can be resolved.

Do localized resonances exist in BLG? At first glance, the large flat density of states in BLG would result in the fast decay of such a state. However, the recent analysis of barrier transmission problem in bilayer graphene [5] suggests that the coupling to the continuum can be suppressed as a consequence of chirality conservation. For a one-dimensional barrier $U(x)$, the quasimomentum perpendicular to the barrier, p_y , is conserved. For normal incidence, $p_y = 0$, electron and hole continua decouple, and the problem is equivalent to two one-dimensional Schrödinger equations for two massive, non-chiral particles, which differ only by the sign of the potential energy. An attractive potential $U(x) < 0$ hosts at least one bound state at negative energies, for any potential strength. The state is submerged into the continuum of holes, repelled by the potential $-U(x)$. In [5] this phenomenon was referred to as *cloaking*, by analogy with cloaking in optics [8, 9]. Indeed, one cannot probe, e.g., the

occupancy of the level using decoupled hole states coexisting in energy. Away from normal incidence, however, the coupling between electron and hole states is proportional to p_y , so that the localized level acquires finite width $\propto p_y^2$, and thus is turned into a resonant barrier state which can contribute to the transmission [10]. Thus, a cloaked state appears as a singular point at $p_y = 0$. Another manifestation of decoupling between electrons and holes in quantum dots in graphene was mentioned in the context of quantum dots in BLG [11].

In this Letter, we show that cloaked states in BLG can be hosted by a local, circularly symmetric potential. The cloaking occurs in the s -wave channel, which serves as an analogue of the normal incidence channel in the barrier transmission problem. Thus, the cloaking relies on a discrete quantum number, which results in perfect isolation of the cloaked state from the continuum, and gives a truly discrete level. Unlike the case of one dimension, however, we also find that the bound states only occur if the potential exceeds a certain critical strength. We also consider how the cloaked states decay due to trigonal warping, and show that their resonant width is less than 1meV. We also discuss potential experimental signatures of cloaked states.

To analyze the dynamics of charge carriers in BLG, we introduce the following single-particle Hamiltonian[2]

$$\hat{H} = \frac{1}{2m^*} \begin{pmatrix} 0 & (\hat{p}_x - i\hat{p}_y)^2 \\ (\hat{p}_x + i\hat{p}_y)^2 & 0 \end{pmatrix} + U(x, y) , \quad (1)$$

where $\hat{p}_{x,y} = -i\hbar\partial_{x,y}$ are the standard momentum operators, $m^* \approx 0.036m_e$ is the effective mass of charge carriers, and $U(x, y)$ is the confining potential. The matrix Hamiltonian operates on two-component wave functions which represent the two pseudospin states. For free electrons ($U = 0$), the eigenstates of this Hamiltonian give two parabolic dispersion bands, $\epsilon_{\mathbf{k}} = \pm\hbar^2\mathbf{k}^2/(2m^*)$. The chirality of charge carriers is reflected in the non-trivial phase of the momentum combination $(\hat{p}_x + i\hat{p}_y)^2$. In particular, this leads to the relative momentum-dependent phase between the two components of a plane wave: $\Psi_2 = \pm e^{-2i\phi_{\mathbf{k}}}\Psi_1$, where $\phi_{\mathbf{k}}$ is the azimuthal angle of the wavevector \mathbf{k} .

We analyze the case of a circularly symmetric potential, introducing the polar coordinates: $x = r \cos \phi$, $y = r \sin \phi$, so that $U = U(r)$. The quantum states can be characterized by their angular momentum quantum number $M = \dots, -2, -1, 0, 1, 2, \dots$, which takes integer values. We shall represent the wave function as a superposition of two components of

opposite chirality described by the two amplitudes, $u_M(r)$ and $v_M(r)$:

$$\Psi_M(r, \phi) = e^{iM\phi} \begin{pmatrix} e^{-i\phi}[u_M(r) + v_M(r)] \\ e^{i\phi}[u_M(r) - v_M(r)] \end{pmatrix} . \quad (2)$$

Note that the magnetic number for the two pseudospin components differ by two; this is characteristic of bilayer graphene. Let us substitute the ansatz (2) into Schrödinger equation $\hat{H}\Psi_M = \epsilon\Psi_M$ with the Hamiltonian (1). In polar coordinates, the differential operators $\partial_x \pm i\partial_y$ take the form $e^{i\phi} [\partial_r \pm \frac{i}{r}\partial_\phi]$. The chiral components $u_M(r)$ and $v_M(r)$ can then be separated by calculating the sum and difference of the two equations:

$$\begin{aligned} [\epsilon - U] u_M &= -\frac{\hbar^2}{2m^*} \left[\hat{\mathcal{D}}_M u_M - \frac{2Mv'_M}{r} \right] , \\ -[\epsilon - U] v_M &= -\frac{\hbar^2}{2m^*} \left[\hat{\mathcal{D}}_M v_M - \frac{2Mu'_M}{r} \right] , \\ \text{where } \hat{\mathcal{D}}_M u &\equiv u'' + \frac{u'}{r} + \frac{M^2 - 1}{r^2}u , u' \equiv \frac{du}{dr} . \end{aligned} \quad (3)$$

The terms proportional to $2M/r$ describe the coupling between $u_M(r)$ and $v_M(r)$ and makes this system equivalent to a biharmonic equation. Interestingly, the equations decouple in the *s*-wave channel, $M = 0$:

$$\begin{aligned} \epsilon u_0 &= -\frac{\hbar^2}{2m^*} \hat{\mathcal{D}}_0 u_0 + U(r)u_0 , \\ -\epsilon v_0 &= -\frac{\hbar^2}{2m^*} \hat{\mathcal{D}}_0 v_0 - U(r)v_0 . \end{aligned} \quad (4)$$

These equations resemble the ones considered in [5], in the limit of normal incidence. The two chirality components are described by the two decoupled amplitudes $u_0(r)$ and $v_0(r)$; the confining potential $U(r)$ is attractive for one component and is repulsive for the other. The differential operator $\hat{\mathcal{D}}_0$ on the right-hand side of Eqs.(4) is identical to the radial part of the Laplacian operator in two dimensions in the angular momentum channel with $M = \pm 1$, i.e., in the *p*-channel. Therefore, the solutions in the *s*-wave channel for bilayer graphene could be constructed from *p*-wave solutions of the Schrödinger equation for a massive non-chiral particle in two dimensions. (Alternatively, one can map the wave function onto the *s*-state in four dimensions, by the change of variable $u_0(r) = rw_0(r)$, which brings the kinetic energy to the form $w_0'' + 3w_0'/r$.) For positive chirality states described by $u_0(r)$ the potential in the Schrödinger equation is $U(r)$, and the energy is ϵ ; for states in the opposite chirality channel these quantities change sign. Thus, the two components, $u_0(r)$ and $v_0(r)$ describe the two *s*-wave subbands of electron-like and hole-like states, respectively.

Before employing this mapping, let us recall the properties of bound states for a massive non-chiral particle. In dimensions less than or equal to two, a bound state in the s -channel exists for an arbitrary weak potential; however, the binding energy decreases with increasing dimension [12]. Bound states in higher momentum channels exist only if the potential is sufficiently strong, so that it can overcome quantum zero-point motion energy and the centrifugal barrier. The massive particle in more than two dimensions can be confined by a negative potential $U(r)$ if its strength exceeds a certain critical value, of the order of the zero-point energy in the potential. For a three-dimensional square well [13] of radius a ($U(r) = -U_0$ for $r < a$), this value is $U_{0,\text{cr}} = \frac{\pi^2 \hbar^2}{8m^* a^2}$. The same analysis can be carried over for a bound state in the p -channel in two dimensions: the bound state becomes detached from the continuum when the wave function inside the well reaches its maximum at the well boundary. On the other hand, the wave function in the p -channel regular at $r = 0$ must be proportional to r . For a rectangular well, the wave function inside the well is $J_1(qr)$, where $q = \sqrt{2m^* U_0}/\hbar$ is the wavenumber inside the well, and $J_1(x)$ is the first order Bessel function. This function reaches its first maximum at $x = 1.84$, which gives the critical well depth $U_{0,\text{cr}} = 1.70 \hbar^2/(m^* a^2)$. The estimate $U_{0,\text{cr}} \sim \hbar^2/(m^* a^2)$ is valid irrespectively of the details of the well profile.

We can now state the central finding of this paper: discrete bound states exist in the electron spectrum of bilayer graphene when the potential $U(r)$ exceeds the critical strength: if it hosts a bound state in the p -channel for the massive non-chiral particle in two dimensions, it can also host a cloaked bound state in BLG. The critical potential strength is of the order of the kinetic energy of quantum zero-point motion, $\hbar^2/(m^* a^2)$, where a is the radius of the potential. Note, however, that the bound state in bilayer graphene occurs irrespective of the sign of the potential energy, due to the particle-hole symmetry. For an attractive potential, the cloaked state is split off the electron continuum and submerged into the hole continuum, while a repulsive potential gives rise to a hole-like state.

Let us now discuss the physical situations in which the cloaked states can occur. It is very natural to check if cloaked states can be hosted by charged impurities. One can consider the cloaking by the Coulomb potential $U(r) = -Ze^2/\varkappa r$, induced by the charge Ze , where \varkappa is the effective dielectric constant of graphene and its environment. For such a potential, infinitely many Rydberg-like bound states exist at arbitrarily small charge Z in all momentum channels. In principle, a Coulomb potential acting on electrons in bilayer

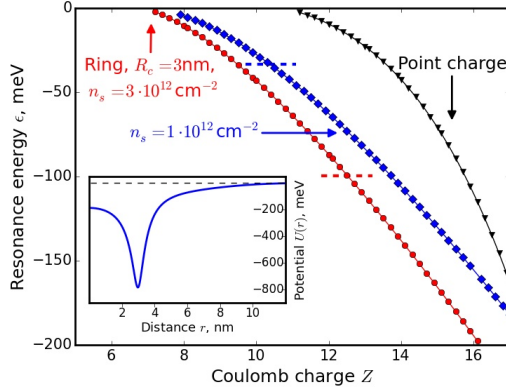


FIG. 1. The position of the cloaked level as a function of the total charge for the two distributions: (i) point-like charge (black), (ii) charged ring (red, blue). One can see that the cloaking is facilitated by deconcentrating the charge. The screening is slightly affected by the background charge density n_s : for the lower charge density (the blue curve), the screening is enhanced at short distances owing to the wavevector dependence of the polarization operator [15]. This results in smaller energy of the cloaked state. The dashed lines indicate the position of the Fermi level. Inset: the potential energy profile $U(r)$ in the ring configuration for the background charge density $n_s = 3 \cdot 10^{12} \text{ cm}^{-2}$.

graphene would also host a hydrogen-like spectrum of cloaked states [14], with energies $\epsilon_n = -E_R Z^2 / (n+3/2)^2$, with Rydberg energy $E_R = \frac{1}{2} m^* e^4 / (\varkappa \hbar)^2$. For bilayer graphene on a SiO_2 substrate ($\varkappa = 2.5$), the energy of the lowest cloaked state would be $\epsilon_0 = -35 \text{ meV}$, due to small effective mass. However, unlike the case of donor states in semiconductors, an external Coulomb potential is effectively screened in bilayer graphene due to the non-vanishing density of states and $N = 4$ fermion flavours. The corresponding Thomas-Fermi screening radius, $\hbar^2 \varkappa / (N m^* e^2) \approx 0.37 \text{ nm}$ is therefore shorter than the Bohr radius $\hbar^2 \varkappa / (m^* e^2) \approx 1.5 \text{ nm}$. The screening by charge carriers in BLG is mostly similar to Thomas-Fermi screening [15], except at distances shorter than the Fermi wavelength, where the response is larger by the factor of $\log 4 \approx 1.4$. This response function can be employed to find the potential induced by a point charge, and then solve Eq. (4) for $u_0(r)$ numerically for different values of the Coulomb charge Z . The resulting dependence of the cloaked level position on Z is shown as the black curve in Fig. 1. The cloaked state exists if Z exceeds the critical value $Z_c \approx 12$. Therefore, it is very unlikely that cloaked states arise as donor or acceptor states due to

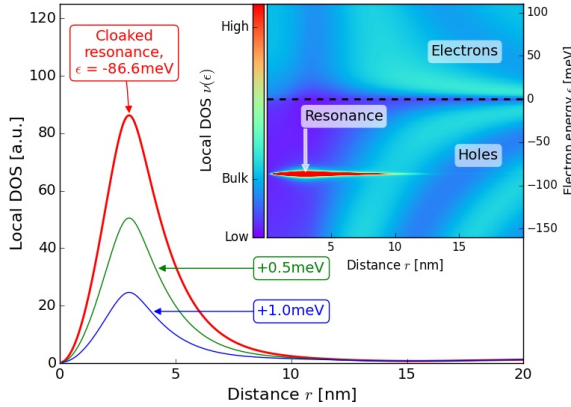


FIG. 2. The Local density of electronic states (LDOS) in quantum corral formed by a ring of charged impurities (3nm in radius, total charge $Z = 12$, background electron density $n_s = 3 \cdot 10^{12} \text{cm}^{-2}$) was obtained by solving Eq.(3) numerically for all channels with $|M| < 10$. The trigonal warping contributions were included for the $M = 0, 3, -3$ channels. The LDOS is shown in the units of its bulk value, $\nu_0 = m^*/(2\pi\hbar^2)$. Near the resonant energy, the LDOS exhibits a sharp peak at $\epsilon = -86\text{meV}$ that represents the probability distribution in the cloaked state. The peak dominates over the surrounding continuum due to its small width, 0.64meV. Inset: the LDOS as a function of energy and the distance away from the center of the corral. The resonant peak is seen as a sharp streak superimposed onto the smooth interference fringes formed by incident and repelled waves in the hole continuum.

charged impurities. The culprit is the repulsion by a centrifugal barrier in the p -state, which prevents the particle from reaching the attractive core of the potential.

The estimate for the critical potential strength, $U_{\text{cr}} \sim \hbar^2/(m^*a^2)$, shows that cloaked states can arise in smooth potentials with a large characteristic distance a . For example, if $a = 10\text{nm}$, the critical strength is estimated to be of the order of 50meV. One can also notice that distributing the positive charge rather than concentrating it at a single point is a way to get around the centrifugal barrier. This suggests a better way to engineer cloaked states. One can create a large cluster of charge impurities by manipulating them with the tip of a scanning microscope. Arranging the impurities into a charged ring (such as a quantum corral [16]), one can lower the required threshold. For example, for impurities placed around the ring of 3nm radius, the simulations give a lower value of the critical charge, $Z_c = 7$, weakly dependent on the background electron density, as shown by the red and blue curves

in Fig. 1. It should be also possible to engineer cloaked states via gating a BLG sample locally, e.g, with the tip of a scanning tunneling microscope [17].

To detect the cloaked resonance, one can measure the local density of states (LDOS) via scanning tunneling microscopy measurements. The LDOS can be defined in terms of the wave functions $(u_{M,\epsilon}(r), v_{M,\epsilon}(r))$ at a given energy ϵ as $\nu(\epsilon, r) \propto \text{sum}_M[u_{M,\epsilon}^2(r) + v_{M,\epsilon}^2(r)]$. To show how the bound state could reveal itself in STM measurements, we have calculated the LDOS numerically, including the effects of RPA screening. The decay due to trigonal warping (see below) was included as Lorentzian broadening of the level. Figure 2 shows the LDOS in the vicinity of a charged ring with total charge $Z = 12$. The resonant contribution can be seen as a sharp fin at $\epsilon_c \approx -86\text{meV}$ sticking out of the hole continuum.

We now turn to the issue of stability of cloaked states. Deviations of the kinetic energy from the chiral form (1) results in the decay of the bound states. The most important next-order contribution to the kinetic energy is the trigonal warping term [2]:

$$H_w = v_3 \begin{pmatrix} 0 & \hat{p}_x + i\hat{p}_y \\ \hat{p}_x - i\hat{p}_y & 0 \end{pmatrix}, \quad (5)$$

where the parameter $v_3 \approx 6 \cdot 10^4 \text{m/s}$. The warping breaks chirality and angular momentum conservation. Applying H_w to the wave function (2), we find

$$H_w \begin{pmatrix} e^{-i\phi} \\ e^{i\phi} \end{pmatrix} u_0(r) = -i\hbar v_3 \left[u'_0 - \frac{u_0}{r} \right] \begin{pmatrix} e^{2i\phi} \\ e^{-2i\phi} \end{pmatrix}. \quad (6)$$

Hence, the cloaked $M = 0$ state could decay into $M = \pm 3$ continuum states. This decay, however, is partially suppressed by two effects. Firstly, the wave function with large angular momentum is suppressed near the origin $r = 0$ due to the centrifugal barrier. Second, the continuum state, unlike the cloaked state, is repelled by the potential $-U(r)$. Near the critical threshold, when the resonant state is shallow, the dominant effect is due to the centrifugal potential. A simple estimate of the resulting resonant width can be found with the help of Fermi's golden rule. Let us assume, for simplicity, that we consider the state near the cloaking threshold. This state can be described by a shallow wave function, independent of the profile of the potential. For the p -channel, the decaying shallow-state wave function is proportional to the first-order Macdonald function $K_1(\kappa r)$. The parameter κ is related to the energy of the cloaked state: $\epsilon_c = -\frac{\hbar^2 \kappa^2}{2m^*}$. The outgoing wave that coexists at the same energy has the wavenumber κ , and the corresponding wave function in the $M = 3$ channel

can be written in terms of Bessel functions $J_{M\pm 1}(\kappa r)$. The properly normalized initial and final states are

$$\begin{aligned}\Psi_{\text{in}} &= \frac{\kappa K_1(\kappa r)}{\sqrt{4\pi \log \frac{1}{\kappa a}}} \begin{pmatrix} e^{-i\phi} \\ e^{i\phi} \end{pmatrix}, \\ \Psi_{\text{out}} &= \sqrt{\frac{\kappa}{4R}} \begin{pmatrix} J_2(\kappa r)e^{2i\phi} \\ J_4(\kappa r)e^{4i\phi} \end{pmatrix},\end{aligned}\quad (7)$$

where R is a large normalization radius for continuum states. Applying recursive relations between Bessel functions and known integrals [18], one can find the transition matrix element:

$$V \equiv \langle \Psi_{\text{out}} | \hat{H}_w | \Psi_{\text{in}} \rangle = -i\hbar v_3 \sqrt{\frac{\pi\kappa}{16R \log \frac{1}{\kappa a}}}. \quad (8)$$

The density of final states in a given angular momentum channel is $\nu_{M=\pm 3} = (R/\pi)(dk/dE) = (Rm^*)/(\pi\hbar^2\kappa)$. The golden rule formula then gives the decay width as

$$\Gamma = 2 \times \frac{2\pi}{\hbar} |V|^2 \nu_{M=3} = \frac{\pi}{4 \log \frac{1}{\kappa a}} m^* v_3^2 \quad (9)$$

(we have included both momentum channels here). Thus, we see that the broadening of the cloaked state is only weakly dependent of its energy, and is given by the quantity $(\pi/4)m^*v_3^2 \approx 0.6\text{meV}$. Therefore, the warping becomes insignificant when the energy of the cloaked state exceeds this value. By dimensional arguments, this estimate should hold, by the order of magnitude, irrespective of the details of the well $U(r)$.

One should also bear in mind that transverse electric fields can open a gap in bilayer graphene [19]. The gap Δ violates chirality conservation, and gives the resonance a finite width, $\Gamma \sim \Delta^2/\epsilon_c$; the resonance is quenched if the gap is larger than its energy ϵ_c . Thus, the resonance can be controlled by a transverse field, and this can be potentially employed to identify the signature of cloaked resonances in the experimental data. The cloaked state can be also destroyed by magnetic field. Indeed, the effect of the magnetic field B amounts to shifting the angular momentum. The resonance is destroyed when the magnetic flux through the cloaked orbit becomes of the order of one flux quantum, or when the cyclotron energy is comparable with the energy of the cloaked state. This analysis also shows that it may be desirable to avoid non-uniform strain in the cloaked region to minimize the detrimental effects of pseudomagnetic fields [20].

An interesting open question is the role of symmetry in this problem. Cloaked states have been found here for strong potentials with rotational symmetry; earlier, cloaked states were identified for an arbitrarily weak potentials with translational symmetry[5]. The two solutions share a common feature: the two components of the wave function of the cloaked states are complex conjugate to each other: $\Psi = (\psi(x, y), \pm\psi^*(x, y))$. Indeed, if the Hamiltonian admits solutions of this type, one can show that the two chirality components are decoupled. Whether this can occur in other geometries, in particular, non-symmetric ones, perhaps, with a different potential strength threshold, is not known to the author.

Thus, we have shown that chirality of quasiparticles in bilayer graphene results in unconventional bound states that do not hybridize with the surrounding hole continuum. Such states occur if the confining potential exceeds the quantum zero-point motion energy: $|U| > \hbar^2/m^*a^2$. The cloaking can be implemented with both attractive and repulsive potentials. Trigonal warping converts these states into resonances of finite width, transverse electric and magnetic fields can be employed to quench these states. We predict that such states could be engineered in large clusters of charged impurities, and probed by scanning tunneling microscopy experiments. The author would like to thank L.S.Levitov, V.I.Falko, and P.Brouwer for useful discussions. This research was supported by EPSRC/HEFCE No. EP/G036101.

- [1] A. H. Castro Neto et al, Rev. Mod. Phys. **81**, 109 (2009).
- [2] E. McCann, V. I. Falko, Phys.Rev.Lett. **96**, 086805 (2006).
- [3] E. McCann and M. Koshino, Rep.Progr.Phys. **76**, 056503 (2013), and references therein.
- [4] M. I. Katsnelson, K. S. Novoselov, A. K. Geim, Nature Physics **2**, 620 (2006).
- [5] N. Gu, M. Rudner, and L. S. Levitov, Phys. Rev. Lett. **107**, 156603 (2011).
- [6] A. V. Shytov, M. I. Katsnelson, L. S. Levitov, Phys.Rev.Lett. **99**, 246802 (2007).
- [7] Y. Wang et al, Science **340**, 734 (2013).
- [8] J. B. Pendry, D. Schurig, and D. R. Smith, Science **312**, 1780 (2006).
- [9] U. Leonhardt, Science **312**, 1777 (2006).
- [10] L. C. Campos et al, Nature Communications **3**, 1239 (2012).
- [11] A. Matulis and F. M. Peeters, Phys. Rev. B **77**, 115423 (2008).

- [12] L. D. Landau and E. M. Lifshitz, *Quantum Mechanics: Non-Relativistic Theory*, Sec.45, Vol. 3 (3rd ed), Pergamon Press (1977).
- [13] ibid., Sec.33.
- [14] B. Zaslow and M. E. Zandler, Am. J. Physics **35**, 1187 (1967).
- [15] E. H. Hwang and S. Das Sarma, Phys. Rev. Lett. **101**, 156802 (2008).
- [16] M. F. Crommie, C. P. Lutz, and D. M. Eigler, Science **262**, 218 (1993).
- [17] Y. Zhao et al, Science **348**, 672 (2015).
- [18] I. S. Gradstein and I. M. Ryzhik, ed. by A. Jeffrey, *Table of Integrals, Series, and Products* (5th ed), Academic Press, New York (1994), Eqs. 8.473 and 6.521.2.
- [19] Y. Zhang et al, Nature **459**, 820 (2009)
- [20] F. Guinea, M. I. Katsnelson, and A. K. Geim, Nat. Phys. **6**, 30 (2010).